Understanding the Influence of Polymorphism on Phonon Spectra: Lattice Dynamics Calculations and Terahertz Spectroscopy of Carbamazepine

G. M. Day,*,† J. A. Zeitler,‡,§,|| W. Jones,† T. Rades,‡ and P. F. Taday||

Department of Chemistry, University of Cambridge, Lensfield Road, Cambridge, CB2 1EW, U.K., School of Pharmacy, University of Otago, New Zealand, Cavendish Laboratory, University of Cambridge, Cambridge, U.K., and TeraView Limited, St. John's Innovation Park, Cowley Road, Cambridge, CB4 0WS, U.K.

Received: September 25, 2005; In Final Form: November 3, 2005

Rigid molecule atomistic lattice dynamics calculations have been performed to predict the phonon spectra of the four polymorphs of carbamazepine, and these calculations predict that there should be differences in the spectra of all four forms. Terahertz spectra have been measured for forms I and III, and there are clearly different features between polymorphs' spectra, that are accentuated at low temperature. While carbamazepine adopts the same hydrogen bonded dimers in all of its known polymorphs, the calculations show that differences in packing arrangements of the dimers lead to changes in the frequency ranges for each type of hydrogen bond vibration, giving a physical explanation to the observed differences between the spectra. Although the agreement between calculated and observed spectra does not allow a definitive characterization of the spectra, it is possible to make tentative assignments of many of the observed features in the terahertz region for the simpler form III; we can only make some tentative assignments of specific modes in the more complex spectrum of form I. While harmonic rigid molecule lattice dynamics shows promise for understanding the differences in spectra between polymorphs of organic molecules, discrepancies between observed and calculated spectra suggest areas of improvement in the computational methods for more accurate modeling of the dynamics in molecular organic crystals.

1. Introduction

The relatively unexplored central part of the terahertz spectrum (60 GHz−4 THz = 2−133 cm^{-1}) is a powerful tool for studying the dynamics of molecules in crystals. The frequencies examined in this range are at lower energies than most of the internal vibrations of molecules (e.g., bond stretching and angle bending), instead corresponding to translations and librations of molecules which yield information on intermolecular interactions. Recent developments in ultrafast laser systems and semiconductor devices have made this region of the electromagnetic spectrum much more accessible; measurements can now be performed much more quickly and conveniently, with no need for cryogenic cooled detectors.[1,2]

As there are many potential applications of terahertz spectroscopy, there is a growing need for a fundamental understanding, at the molecular level, of the motions corresponding to absorptions in the terahertz spectra of molecular crystals, i.e., to characterize the molecular motions involved in the phonon modes. The probing of intermolecular interactions makes terahertz spectroscopy an ideal method for the study of polymorphism, where a molecule exhibits the ability to pack in two or more crystal forms.[3] The control, detection, and an understanding of polymorphism are of particular importance in the pharmaceutical industry, where a change in crystal form can have drastic implications, both in terms of intellectual property issues and the physicochemical properties of the dosage form. Changes in molecular packing between polymorphs result in differences in intermolecular interactions, which have been shown to lead to dramatic differences in their terahertz spectra;[1] this is promising for the use of terahertz spectroscopy for the rapid identification of polymorphic content in crystalline materials.[2] There is clearly a need for investigations of the differences in terahertz vibrational spectra between polymorphs. The two main motivations of the current study are (i) to assess the ability of rigid molecule, harmonic lattice dynamics to characterize the terahertz spectra of organic molecular crystals and (ii) to examine the differences in low frequency vibrations between polymorphs. We chose the molecule carbamazepine as a model system for these purposes.

Carbamazepine, used in the treatment of epilepsy, is polymorphic; four anhydrous polymorphs are known (which we refer to as forms I − IV, Figure 1), as well as a lengthy list of solvates.[4] As a relatively simple drug compound, carbamazepine has been the subject of many experimental and computational studies, including extensive polymorph and solvate screening,[4−6] as well as computational studies of the real and hypothetical (computer-generated) polymorphs.[6,7] All four known polymorphs of carbamazepine share a common hydrogen bonding motif (Figure 1), with pairs of molecules joined by two N−H···O=C amide−amide hydrogen bonds. The resulting dimers lie on inversion centers in forms II (spacegroup $R\bar{3}$), III ($P2_1/c$), and IV ($C2/c$). In the $P\bar{1}$ form I, there are four symmetrically independent molecules ($Z' = 4$), forming three independent dimers; two dimers hydrogen bond across crystallographic inversion centers, while the third is formed by the remaining two molecules and sits on a general position. The lower

* gmd27@cam.ac.uk.
† Department of Chemistry, University of Cambridge.
‡ University of Otago.
§ Cavendish Laboratory, University of Cambridge.
|| TeraView Limited.

10.1021/jp055439y CCC: $33.50
Published on Web 12/15/2005

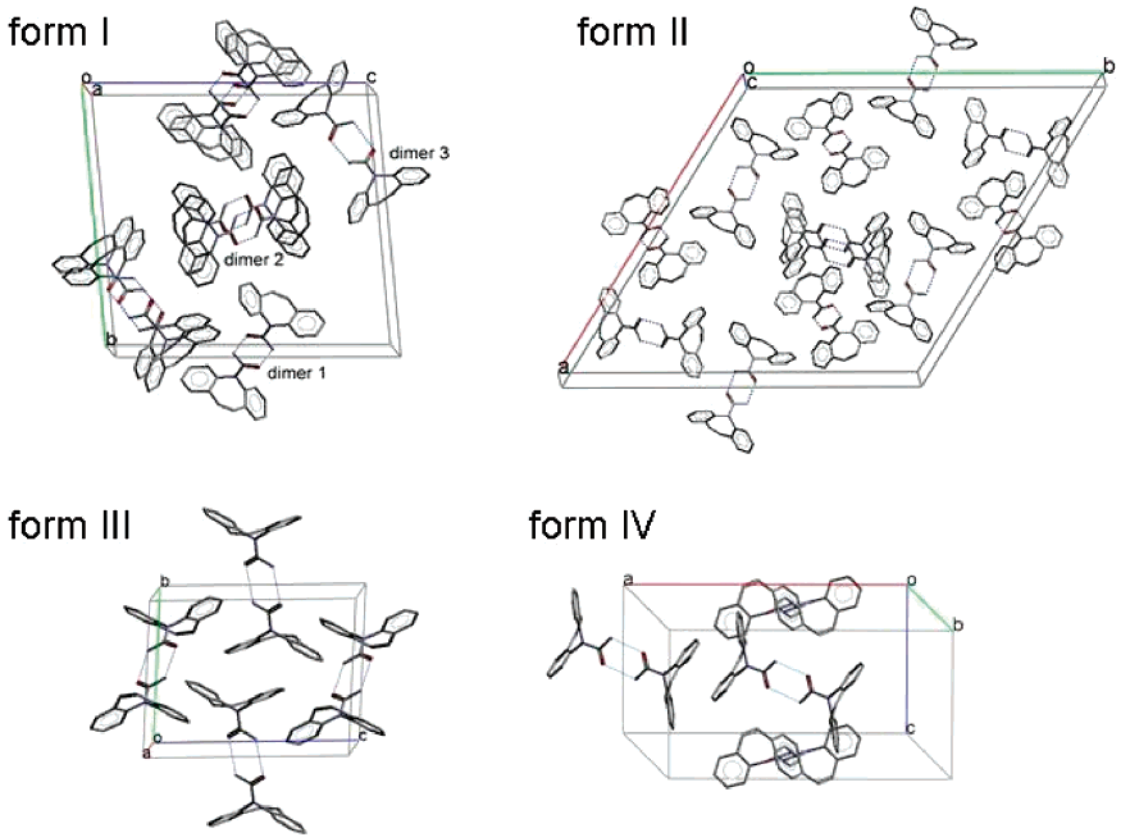

Figure 1. Packing diagrams of the four known polymorphs of carbamazepine. Dashed blue lines indicate hydrogen bonds. The three independent hydrogen-bonded dimers are labeled in form I. Hydrogen atoms are omitted for clarity.

symmetry of form I results in a more complex phonon spectrum than those of the others. As the strong hydrogen bonding is the same in all four crystal structures, the observed polymorphism results from the alternative possibilities of packing these dimers into a stable crystal structure: forms I and II have similar packing of dimers, with offset $\pi-\pi$ stacking of the aromatic rings as the main interaction between neighboring dimers. Forms III and IV show a different packing of the dimers, where aromatic rings form both $\pi-\pi$ stacking and edge-to-face contacts in an interlocked packing arrangement. Although we only collected spectra for forms I and III, calculations were performed on all four known polymorphs, so that we could examine the effect of packing in each polymorph on the calculated vibrational modes and anticipate features that would be seen in the spectra of forms II and IV.

2. Methodology

2.1. Materials and Sample Preparation. Carbamazepine (5H-dibenz[*b*,*f*]azepine-5-carboxamide) was obtained from Sigma-Aldrich (Poole, UK). The commercial product was supplied as form III ($P2_1/c$) and used without further purification. By heating form III to 443 K for 2 h, the triclinic form I was obtained, as described by Lefebvre et al.[8] and McMahon et al.[9] Polyethylene (PE) powder (Inducos 13/1, particle size <80 μm) was purchased from Induchem (Volketswil, Switzerland). A 20 mg portion of the respective forms was physically mixed with 400 mg PE powder and pressed into a 13 mm diameter pellet using a die press (Specac, Orpington, UK). For the reference pellets, 400 mg of PE powder was used.

2.2. Measurements. The sample pellets were attached to the coldfinger of a modified Optistat-CF cryostat (Oxford Instruments, Witney, UK) with poly(tetrafluoroethylene) (PTFE) windows. Thermal contact of the pellet to the coldfinger was ensured by applying Apiezon N grease (M&I Materials, Manchester, UK). Using liquid He, the samples were cooled to 7 K. The sample temperature was validated using a calibrated reference silicon diode temperature sensor (DT-670, Lake Shore Cryotronics, Westerville, USA). All spectra were recorded in transmission on a TPI spectra 1000 spectrometer (TeraView, Cambridge, UK) at an instrument resolution of 1 cm^{-1} over the range 2−120 cm^{-1}.[10] For each spectrum, 900 scans were co-added resulting in a total acquisition time of 30 s per spectrum. Sample and reference spectra were recorded at 7 K and intermediate temperatures up to 300 K. The time-domain waveform of the sample and reference was transformed into the frequency domain by fast Fourier transformation (FFT). Factor 2 zerofilling and Blackman−Harris 3-term apodization were applied. Using the sample and reference spectra, the absorbance spectra were calculated. The OPUS 4.2 program (Bruker Optik, Ettlingen, Germany) was used for data acquisition and spectrum processing. Only the polymorphic forms I and III were studied spectroscopically, as these could be easily prepared and remained stable for the low temperature measurements, which are vital for comparison to the calculated spectra.

2.3. Computational Methods. *Lattice Dynamics.* The theory of lattice dynamics was developed by Born and Huang[11] for a lattice of point masses, and this general theory was later adapted for rigid molecules,[12,13] with translational and rotational degrees of freedom. The rigid molecule approximation assumes a separation between inter- and intramolecular vibrational modes, simplifying the analysis of the vibrations in molecular crystals, which are described in terms of molecular librations and translations. In the harmonic approximation,

the resulting equations are

$$\omega^2(\mathbf{k})w_\tau(M|\mathbf{k}) = \sum_{\tau',N} D^{MN}_{\tau\tau'}(\mathbf{k})w_{\tau'}(N|\mathbf{k}) \quad (1)$$

where $\omega(\mathbf{k})$ is the frequency of vibration at wavevector $\mathbf{k}$ and $w_\tau(M|\mathbf{k})$ is a mass-weighted displacement of molecule M along τ, a molecular translation ($\tau = 1-3$) or rotation about a principal inertial axis ($\tau = 4-6$). For comparison to optical spectroscopy, only the wavevector $\mathbf{k} = 0$ must be considered; eigenvalues and eigenvectors were determined by diagonalization of the dynamical matrix:

$$D^{MN}_{\tau\tau'}(\mathbf{k}) = (\mathbf{M}_{\tau,M}\mathbf{M}_{\tau',N})^{-1/2}\sum_{l'}\Phi^{0l'}_{\tau\tau'}(MN)\exp(i\mathbf{k}\cdot\mathbf{r}^{l'}) \quad (2)$$

Here, $\mathbf{M}$ are the molecular masses ($\tau = 1-3$) and moments of inertia ($\tau = 4-6$). $\Phi^{0l'}_{\tau\tau'}(MN)$ is the matrix of second derivatives with respect to the displacements of molecule M (in the reference unit cell) and molecule N (in unit cell l') along τ and τ', respectively, with the vector $\mathbf{r}^l$ joining atoms in the reference unit cell to those in unit cell l. Eigenvectors were examined to determine the symmetry of each normal mode, and the molecular motions were visually inspected using the program RUDOLPh.[14]

The frequency separations between phonon modes are often small, so the interpretation of experimentally determined spectra can be greatly aided by calculated absorption intensities. Under the usual assumption that the transition dipole moment is for the fundamental transition (i.e., between the ground and the first excited state), relative intensities of the phonon modes were calculated from

$$I_\lambda \propto g_\lambda|\partial P/\partial Q_\lambda|^2 \quad (3)$$

where $\partial P/\partial Q_\lambda$ is the unit cell dipole induced by the normal mode Q_λ, of degeneracy g_λ.

Molecular Geometry and Model Potential. Calculations were performed on each of the four known polymorphs of carbamazepine, taking molecular structures from the X-ray determined coordinates; the structure with lowest *R*-factor for each polymorph was taken from the Cambridge Structural Database[15] (form I CSD reference code CBMZPN11,[16] determined at $T = 158$ K; form II CBMZPN03,[17] room temperature; form III CBMZPN01,[18] room temperature; form IV CBMZPN12,[19] $T = 158$ K). Lattice energy calculations can be very sensitive to small changes in the assumed molecular geometry,[20] especially the positions of hydrogen atoms involved in hydrogen bonding and other close intermolecular contacts. X-ray determined hydrogen atom positions are often not satisfactorily accurate for modeling purposes, so positions were optimized for the isolated molecule; density functional theory (PW91/DNP in the program Dmol3[21]) partial geometry optimizations were performed for each molecule, fixing all carbon, nitrogen, and oxygen positions at experimentally observed positions while optimizing hydrogen atom positions in isolated molecule calculations. The geometries of these corrected molecular structures were placed in the crystal structures and held fixed for the remainder of the calculations.

The choice of model potential can have an important effect on the calculated phonon frequencies;[22] we used an exp-6 atom−atom description of repulsion−dispersion intermolecular interactions, choosing the W99[23−25] set of empirically derived potential parameters. The calculated frequencies of phonon modes that distort polar interactions, especially the bending of hydrogen bonds, require a high quality model for intermolecular electrostatic interactions.[22] As we want a trustworthy description of the differences between the polymorphs' spectra, we employed an elaborate electrostatic model—a distributed multipole analysis of a wavefunction calculated using the program CADPAC[26] (B3P91/6-31G**). This electrostatic model adequately describes the anisotropy in atom−atom interactions (due to lone pairs, etc) that is required to satisfactorily model the restoring forces for distortions of hydrogen bonds and other polar interactions. Multipoles up to hexadecapole (charge, dipole, quadrupole, octupole, and hexadecapole) were included on each atom.

The crystal structures were lattice energy minimized with this exp-6 + atomic multipoles model within the program DMAREL,[27,28] and phonon frequencies (with corresponding eigenvectors) were calculated at the lattice energy minimum. Charge−charge, charge−dipole, and dipole−dipole terms were summed by Ewald summation, while higher order terms (up to R^{-5}) were summed in direct space, to a 15 Å cutoff between molecular centers of mass; exp-6 interactions were summed to a 15 Å atom−atom cutoff. Quasi-harmonic frequencies, where molecular positions and orientations were relaxed with the lattice parameters fixed at experimentally determined values, were also calculated. These can account for some temperature effects and aid in the characterization of phonon spectra[22] but did not add to our confidence in describing the carbamazepine spectra, so we only discuss the harmonic calculations (i.e., from fully lattice energy minimized crystal structures).

3. Results and Discussion

Room temperature terahertz spectra of forms I and III of carbamazepine (Figure 2, top spectra) show differences between polymorphs that are significantly more marked than those seen at higher frequency.[29] However, the room temperature spectra show broad features and, while they are adequate for distinguishing between crystal forms, better resolution of the peaks is required for comparison to the lattice dynamics calculations and characterization of the modes. Therefore, samples were cooled, taking spectra at several temperatures down to 7K (Figure 2, bottom spectra). As the temperature is decreased, we observe the expected shifting of the peak positions to higher frequency (sometimes by as much as 7−8 cm^{-1}), as well as a dramatic sharpening of the peaks. For both polymorphs, the very broad features between 80 and 100 cm^{-1} in the room temperature spectra are resolved into several peaks at low temperature. There is similarly improved resolution of individual features across the entire frequency range, so the differences in the spectra between forms I and III are very clear at low temperatures.

3.1. Crystal Structures. All four structures are modeled very well upon lattice energy minimization (Table 1), with changes in unit cell dimensions of less than 2.5% (root mean square (rms) deviations in the lattice parameters *a*, *b*, and *c* of 1.09, 0.20, 0.95, and 1.74% for forms I−IV, respectively). Reorientation of the molecules within the lattice is also acceptably small—typically about 1−2° upon lattice energy minimization.

The lattice energies presented here show that the four polymorphs are close in energy, but these are only a measure of the intermolecular interactions and do not reflect the energetic cost of the distortion from ideal molecular geometry. The molecular geometry is slightly different in the four polymorphs, the main variation being the degree of NH_2 pyramidalization and rotation of the amide group with respect to the ring system; the associated conformational energies and the effects of such differences on the relative stability of the polymorphs have been

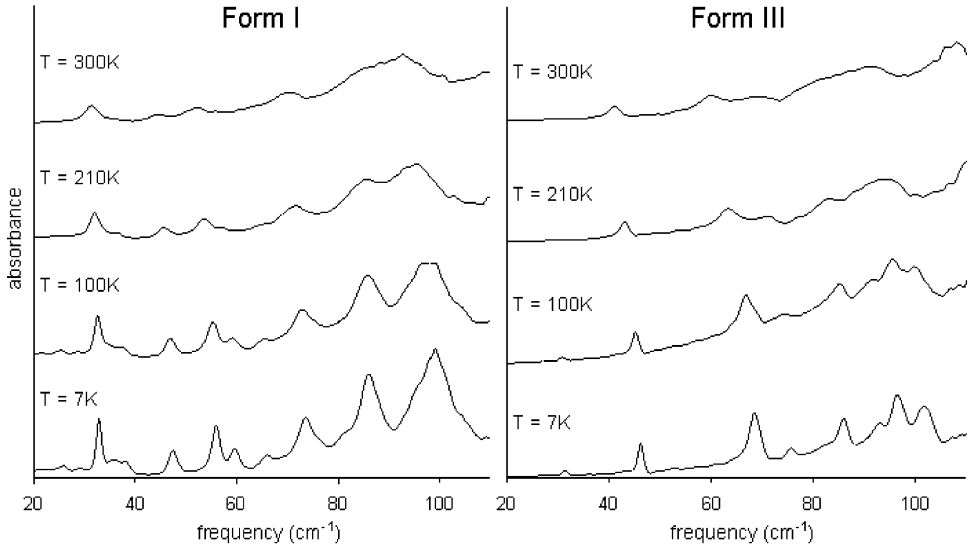

Figure 2. Room and low temperature spectra of carbamazepine forms I (left) and III (right). The spectra are offset in absorbance for clarity.

TABLE 1: Observed (obs) and Lattice Energy Minimized (min.) Unit Cell Parameters, Structural Distortion, and Lattice Energies of the Four Polymorphs of Carbamazepine

	a (Å)	b (Å)	c (Å)	α (degrees)	β (degrees)	γ (degrees)	ρ (g/cm^3)	Θ^a (degrees)	lattice energy (kJ/mol)
				Form I (Spacegroup $P\bar{1}$, Z′ = 4, Z = 8)					
obs	5.171	20.574	22.245	84.12	88.01	85.19	1.339		
min.	5.218	20.914	22.272	84.41	88.27	85.05	1.303	1.12[b]	−122.56
	(+0.92%)	(+1.65%)	(+0.12%)	(+0.34%)	(+0.30%)	(−0.16%)	(−2.69%)		
				Form II (Spacegroup $R\bar{3}$, Z′ = 1, Z = 18)					
obs	35.454	35.454	5.253	90	90	120	1.235		
min.	35.429	35.429	5.270	90	90	120	1.233	2.22	−116.56
	(−0.07%)	(−0.07%)	(+0.33%)				(−0.19%)		
				Form III (Spacegroup $P2_1/c$, Z′ = 1, Z = 4)					
obs	7.529	11.148	15.470	90	116.17	90	1.347		
min.	7.646	11.090	15.495	90	116.57	90	1.335	0.97	−122.36
	(+1.55%)	(−0.52%)	(+0.16%)		(+0.34%)		(−0.85%)		
				Form IV (Spacegroup $C2/c$, Z′ = 1, Z = 8)					
obs	26.609	6.927	13.957	90	109.70	90	1.279		
min.	26.970	6.849	14.299	90	110.66	90	1.253	1.32	−122.78
	(+1.35%)	(−1.12%)	(+2.46%)		(+0.87%)		(−2.03%)		

[a] Θ is the magnitude of the rigid molecule rotation between the starting structure and the lattice energy minimum. [b] The rms average over the rotations of the four independent molecules.

examined in detail in an examination of carbamazepine in the context of crystal structure prediction.[7] Soft molecular degrees of freedom also have an effect on the phonon spectrum, contributing additional modes in the frequency range of interest as well as mixing of inter- and intramolecular modes; the latter effect is not considered in the current work.

3.2. Molecular Vibrations. Zeitler et al.[30] recently presented density functional theory (B3LYP/6-31G**) calculations of the low frequency (<100 cm^{-1}) normal modes of vibration for the isolated carbamazepine molecule, as well as a hydrogen-bonded dimer. Their calculations revealed two molecular vibrations of the isolated molecule in this range—one at 59 cm^{-1} corresponding to a flexing of the ring system and a second just above 80 cm^{-1} resulting from a twisting of the ring system. These shift to 55 and ∼90 cm^{-1} upon dimer formation, where they gain some degree of distortion of the hydrogen bonds (out-of-plane bending in the 55 cm^{-1} mode and twisting in the 90 cm^{-1} mode, see Figure 3). These calculations suggest that absorptions below about 50 cm^{-1} are due entirely to intermolecular motions, while some features seen in the terahertz spectra near 50 and 90 cm^{-1} must arise from *intra*molecular distortions, which might mix with the rigid molecule motions.

3.3. Rigid Molecule Modes. All of the calculated rigid body molecular motions at $\mathbf{k} = 0$ are found in the range from about 20 to 130 cm^{-1}, and these are tabulated for each polymorph in Table 2. These calculations reveal differences in both the magnitude and the range of rigid molecule frequencies: form I frequencies range from 23 to 115 cm^{-1} with a mean frequency ($\bar{\omega}$) of 64.4 cm^{-1}; form II ranges from 28 to 110 cm^{-1} with $\bar{\omega}$ = 63.7 cm^{-1}; form III ranges from 38 to 118 cm^{-1} with $\bar{\omega}$ = 78.5 cm^{-1}; form IV ranges from 26 to 127 cm^{-1} with $\bar{\omega}$ = 72.9 cm^{-1}. The trend in mean frequency (III > IV > I > II) follows the order of densities (III > I > IV > II) fairly well, but the more interesting variations with differences in molecular packing are only revealed in an analysis of individual modes.

3.4. Rigid Molecule Distortions of the Carbamazepine Dimer. The hydrogen-bonded dimer is the common structural unit across all four polymorphs, so we have analyzed the calculated normal modes in terms of their distortion of this hydrogen bonding. There are seven combinations of either molecular translations or librations that result in a change in the carbamazepine dimer geometry (Figure 3), and we classify these as stretching, bending, twisting, and shearing motions for our analysis. In reality, the calculated eigenvectors represent

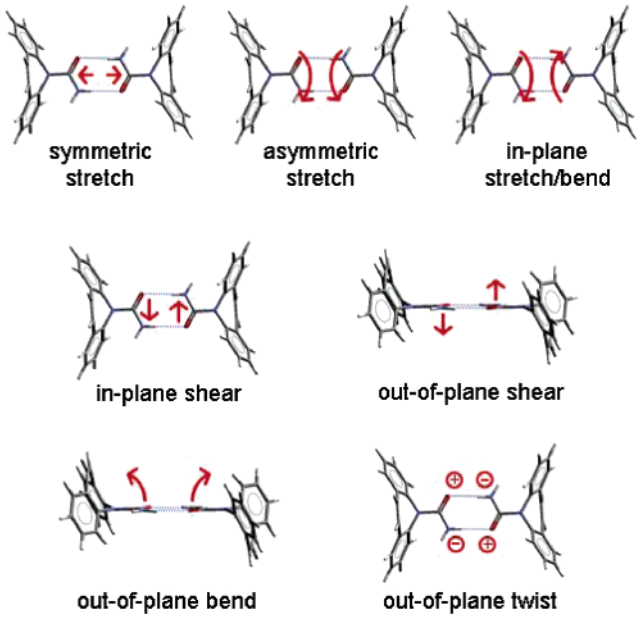

Figure 3. Possible rigid molecule distortions and descriptors of the carbamazepine dimers.

mixtures of these motions, but we find that there is often a dominant contribution to each normal mode and classification according to this dominant distortion is a convenient device for analysis and comparison between polymorphs. Differences in frequency for similar distortions of the hydrogen bonding reflect the differences in packing of the dimers, where the dominant interactions are between the hydrocarbon ring systems.

Vibrational modes corresponding to only a few of the motions shown in Figure 3 are visible in the terahertz spectroscopy experiment; all distortions breaking the inversion symmetry of the dimers (out-of-plane twisting, out-of-plane bending, and asymmetric stretching) generate a dipole in the unit cell and give rise to some peak intensity, depending on the degree of distortion and the relative motions of dimers. The remaining modes of distortion (symmetric stretching, in-plane stretching/bending, and in- and out-of-plane shearing) retain the inversion symmetry, so they do not produce a dipole in the crystal and are inactive in the measured spectra. The exception is form I, where one of the dimers (labeled dimer 3 in Figure 1 and Table 2) is not formed around an inversion center. Therefore, some of the symmetric stretching, in-plane stretching/bending, and shearing motions of dimer 3 can take part in the visible normal modes in this polymorph, though they contribute very little to the transition dipole and, hence, absorption intensity.

The clear differences in the distribution of frequencies between the spectra demonstrate that the spectra are dependent not only on the primary hydrogen-bonding interaction but also on the environment of the dimer and the less directional van der Waals interactions between hydrocarbon moieties. The frequency ranges in which we find the different types of motions are represented in Figure 4. The similarities between forms I and II, and between III and IV, are clear; these are the pairs of polymorphs sharing similar aromatic−aromatic interactions between dimers. The in-plane stretching and bending motions are apparently more hindered by the interlocking combination of $\pi-\pi$ stacking and aromatic edge-to-face contacts in forms III and IV than by the offset $\pi-\pi$ stacking in forms I and II. With the out-of-plane bending and twisting, as well as shearing modes restricted to <100 cm^{-1}, there is a separation of the in-plane stretching/bending from the rest of the types of motion in forms III and IV. In contrast, the frequency ranges of all types of motion overlap in forms I and II, where the stretching vibrations occur at lower frequencies and the out-of-plane bending and twisting modes extend to frequencies above 100 cm^{-1}.

3.5. Sources of Uncertainty. There are three main sources of error in the calculated frequencies: inaccuracies in the model potential, the assumed molecular geometry and rigid molecule approximation, and the harmonic approximation in the lattice dynamics. The first two of these have unpredictable effects on the calculated frequencies. Changes to the repulsion−dispersion or electrostatic model can have great effects on the lattice dynamics,[22] both directly, through changes of the curvature of the intermolecular potentials, and indirectly, through changes to the equilibrium lattice parameters and molecular orientations. We have chosen as reliable a set of exp-6 parameters as possible, along with an elaborate description of the electrostatics, but the main problem with the model potential is the empirical nature of the exp-6 parameters. W99, like many other parameter sets, was parametrized so that lattice energy minimization reproduces the crystal structures of a set of organic molecules, most of which were determined near room temperature. Hence, the resulting potential parameters do not represent the true potential energy surface but accommodate structural changes arising from 300 K of temperature effects (thermal expansion and molecular rearrangement). The harmonic "$T = 0$ K" calculations are, therefore, contaminated by the empirical parametrization procedure, and the effective temperature of the phonon calculations is somewhat indeterminate.

Small changes to the assumed molecular geometry can have a large influence on the calculated energies and structures of molecular crystals[20]—calculated frequencies are presumably also very sensitive. We have tried to take the best available molecular geometries for this work, using low *R*-factor crystal structures and isolated molecule DFT calculations to position the crucial hydrogen atom positions. However, we cannot rule out the effects of small errors in these geometries and the influence of the crystal structure on hydrogen atom positions. At least as important are the frequency shifts caused by mixing of the inter- and intramolecular modes; even for naphthalene, allowing molecular flexibility in the calculations lowers some lattice modes by as much as 5−10 cm^{-1}.[31] Carbamazepine is larger and has softer molecular vibrations than naphthalene, so uncertainties caused by the rigid molecule assumption are probably significant here.

The harmonic approximation influences the lattice dynamics in two ways: thermal expansion, which softens the intermolecular interactions and lowers most frequencies, is not considered, and there is a direct influence of the cubic and higher terms in the expansion of the lattice energy that are dropped in the derivation of eq 1. The ignored terms in the harmonic lattice dynamics have a noticeable effect; for example, at $T = 0$ K, anharmonicity increases the frequency of the phonon modes of naphthalene by up to 3 cm^{-1}.[32] The effect is probably smaller for more strongly bound polar molecules, but it is, nonetheless, a source of uncertainty.

3.6. Comparison with Experiment: Characterization of the Measured Spectra. While the observations summarized in Figure 4 are a useful start to understanding the influence of polymorphism on phonon spectra, an aim of such calculations is the full characterization of measured spectra. We focus here on comparisons to the $T = 7$ K spectra; these better resolved low temperature spectra are more easily analyzed, and bearing in mind our previous comments on the model potential,

TABLE 2: Calculated Rigid Body Modes for Carbamazepine Forms I−IV[a]

Form I[b]

mode (symmetry)	frequency (cm^{-1})	relative intensity	distortion of dimer 1	distortion of dimer 2	distortion of dimer 3
ν_2 (A_u)	24.80	0.161	out-of-plane twist	negligible (dimer translation)	negligible (dimer libration)
ν_4 (A_u)	29.05	0.275	slight out-of-plane twist	negligible (dimer translation)	out-of-plane shear + twist
ν_6 (A_u)	31.39	0.204	slight out-of-plane twist	out-of-plane twist	out-of-plane shear
ν_7 (A_u)	33.48	0.846	out-of-plane twist	out-of-plane bend	slight out-of-plane twist
ν_{10} (A_u)	41.03	0.971	slight out-of-plane twist	out-of-plane twist	out-of-plane twist
ν_{12} (A_u)	43.40	0.348	out-of-plane bend	out-of-plane twist	slight asymmetric stretch
ν_{15} (A_u)	46.98	0.670	out-of-plane twist	out-of-plane twist	out-of-plane twist
ν_{17} (A_u)	49.23	0.050	slight out-of-plane bend	out-of-plane twist	out-of-plane twist
ν_{18} (A_u)	51.44	0.815	slight asymm. stretch	out-of-plane twist	out-of-plane twist + slight symmetric stretch
ν_{19} (A_u)	56.77	0.674	slight asymm. stretch	slight out-of-plane bend	out-of-plane twist
ν_{23} (A_u)	62.17	0.774	slight asymm. stretch	slight asymmetric stretch	out-of-plane twist
ν_{24} (A_u)	63.85	0.396	out-of-plane twist	out-of-plane twist	in-plane shear
ν_{27} (A_u)	71.09	0.269	slight asymm. stretch	out-of-plane bend	in-plane shear + asymmetric stretch
ν_{28} (A_u)	73.10	0.199	large asymm. stretch	slight out-of-plane bend	slight symmetric stretch
ν_{30} (A_u)	75.94	0.449	slight out-of-plane bend	large asymm. stretch	slight out-of-plane twist
ν_{32} (A_u)	81.02	1.000	asymm. stretch	slight asymm. stretch	out-of-plane and in-plane shear
ν_{34} (A_u)	85.70	0.146	out-of-plane bend	out-of-plane bend	in-plane shear
ν_{36} (A_u)	88.96	0.992	out-of-plane bend + asymmetric stretch	out-of-plane bend	out-of-plane bend/twist
ν_{38} (A_u)	91.13	0.555	out-of-plane bend + asymmetric stretch	out-of-plane bend	asymmetric stretch
ν_{41} (A_u)	98.92	0.506	slight asymmetric stretch	slight out-of-plane bend	large in-plane shear
ν_{43} (A_u)	112.22	0.195	slight out-of-plane bend	slight out-of-plane bend	large out-of-plane shear

Form II

mode (symmetry)	degeneracy	frequency (cm^{-1})	relative intensity	distortion of dimer
ν_1 (E_u)	2	27.82	0.573	out-of-plane twist
ν_2 (A_g)	1	32.90	0	out-of-plane shear
ν_3 (E_g)	2	33.69	0	out-of-plane shear
ν_4 (A_u)	1	37.29	0.460	out-of-plane twist
ν_5 (E_g)	2	38.44	0	in-plane shear
ν_6 (E_u)	2	40.28	1.000	out-of-plane twist + slight asymmetric stretch
ν_7 (A_u)	1	41.18	0.738	out-of-plane twist
ν_8 (A_g)	1	41.97	0	slight symmetric stretch (mainly libration of entire dimer)
ν_9 (A_u)	1	55.28	0.128	asymmetric stretch
ν_{10} (A_g)	1	60.80	0	in-plane shear
ν_{11} (E_g)	2	62.05	0	symmetric stretch/in-plane shear
ν_{12} (E_u)	2	62.24	0.964	out-of-plane bend
ν_{13} (A_g)	1	70.08	0	in-plane shear
ν_{14} (E_u)	2	74.76	0.383	out-of-plane bend
ν_{15} (A_u)	1	75.27	0.724	out-of-plane bend
ν_{16} (E_g)	2	76.14	0	in-plane stretch/bend
ν_{17} (E_u)	2	85.81	0.022	out-of-plane bend + asymmetric stretch
ν_{18} (E_g)	2	87.23	0	in-plane stretch/bend
ν_{19} (A_g)	1	89.13	0	in-plane stretch/bend
ν_{20} (A_u)	1	92.26	0.713	asymmetric stretch
ν_{21} (A_g)	1	108.83	0	out-of-plane shear
ν_{22} (E_g)	2	109.51	0	out-of-plane shear

Form III

mode (symmetry)	frequency (cm^{-1})	relative intensity	distortion of dimer
ν_1 (A_u)	37.81	0.001	out-of-plane bend
ν_2 (A_g)	42.96	0	in-plane shear
ν_3 (B_g)	45.87	0	negligible (libration of entire dimer)
ν_4 (B_u)	50.24	0.858	large out-of-plane bend
ν_5 (A_u)	51.22	0.095	out-of-plane twist
ν_6 (A_g)	52.15	0	slight symmetric stretch (mainly libration of entire dimer)
ν_7 (A_g)	57.60	0	large out-of-plane shear
ν_8 (B_g)	61.47	0	large out-of-plane shear
ν_9 (B_g)	77.51	0	large out-of-plane shear + in-plane shear
ν_{10} (B_u)	77.60	0.559	out-of-plane twist
ν_{11} (A_u)	78.82	0.135	out-of-plane bend
ν_{12} (A_u)	81.40	0.073	out-of-plane twist
ν_{13} (A_g)	87.35	0	large out-of-plane shear + in-plane stretch/bend
ν_{14} (B_u)	93.94	0.024	out-of-plane twist
ν_{15} (B_g)	95.46	0	out-of-plane shear
ν_{16} (A_g)	100.06	0	out-of-plane shear + in-plane shear
ν_{17} (B_g)	102.87	0	symmetric stretch
ν_{18} (B_u)	104.61	0.274	asymmetric stretch
ν_{19} (B_g)	112.65	0	in-plane stretch/bend
ν_{20} (A_u)	118.10	1.000	asymmetric stretch
ν_{21} (A_g)	118.30	0	mainly in-plane stretch/bend + slight out-of-plane shear

TABLE 2 (Continued)

Form IV			
mode (symmetry)	frequency (cm^{-1})	relative intensity	distortion of dimer
ν_1 (B_u)	26.01	0.190	out-of-plane twist
ν_2 (A_g)	29.31	0	out-of-plane shear
ν_3 (B_g)	37.37	0	slight out-of-plane shear (mainly libration of entire dimer)
ν_4 (A_u)	44.26	0.226	out-of-plane twist
ν_5 (A_g)	45.25	0	slight out-of-plane shear (mainly libration of entire dimer)
ν_6 (A_u)	54.91	0.001	out-of-plane bend + slight asymmetric stretch
ν_7 (B_u)	55.89	0.292	out-of-plane twist
ν_8 (B_g)	57.35	0	out-of-plane shear + in-plane shear
ν_9 (B_g)	62.79	0	in-plane shear
ν_{10} (A_g)	69.56	0	large in-plane shear
ν_{11} (A_u)	71.68	0.002	slight out-of-plane bend (mainly translation of entire dimer)
ν_{12} (A_u)	73.66	0.266	large out-of-plane bend
ν_{13} (B_u)	78.63	0.350	large out-of-plane bend
ν_{14} (B_g)	88.87	0	large out-of-plane shear
ν_{15} (A_g)	90.97	0	out-of-plane shear + in-plane shear
ν_{16} (B_g)	95.31	0	in-plane stretch/bend + symm. stretch
ν_{17} (A_u)	97.46	0.046	asymmetric stretch
ν_{18} (A_g)	98.44	0	symmetric stretch
ν_{19} (B_u)	100.13	1.000	asymmetric stretch
ν_{20} (B_g)	125.52	0	in-plane stretch/bend
ν_{21} (A_g)	127.24	0	in-plane stretch/bend

[a] Calculated intensities are relative to the strongest peak. [b] IR active modes only (A_u symmetry) are given here. Raman active modes (A_g symmetry) are available in the Supporting Information. The labeling of dimers 1, 2, and 3 is defined in Figure 1.

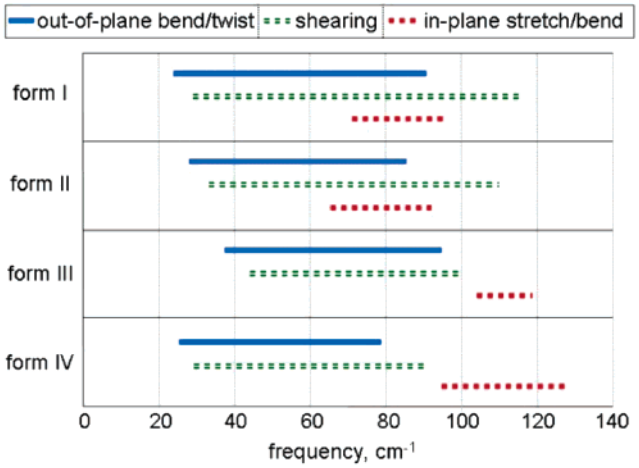

Figure 4. Frequency ranges of the various types of dimer distortion in the four polymorphs of carbamazepine. Only the dominant contribution to each mode is considered in the classification of each calculated mode. All modes (including those not visible in the measured spectra) are included.

harmonic calculations at the lattice energy minima should correspond more closely to the low temperature observations.

Particularly significant is the fact that the calculated intensities vary by up to a factor of 1000, providing important information for the interpretation of observed spectra; the features in the measured spectra show a similar variation in intensity. The baseline intensity that is clear in Figure 2 is a combination of factors whose functional form is not entirely known. However, most of the effects are due to Rayleigh scattering, as the wavelength of the light approaches the particle size in the sample. For the analysis of the spectra, we subtracted an empirical baseline correction of the power function form (intensity $= A \cdot \omega^y$), taken to fit through the first few troughs in the low temperature spectra; the parameters A and y were fitted simultaneously to the 7 K spectra of forms I and III. Those features that are well enough resolved were then integrated to obtain intensities to compare to our calculations (Table 3).

First, we notice that the calculations do predict the general features of the terahertz spectra (Figure 5): reasonably intense peaks are found below 40 cm^{-1} for form I, while form III shows only one weak absorption in this region. Similarly, only weak features are present in the 50−60 cm^{-1} region of the form III spectrum, while form I shows several peaks of reasonable intensity. Such qualitative features, which could be used to rapidly distinguish between polymorphs, are readily predicted by the calculations.

The frequencies and relative intensities of the individual predicted peaks are not in good enough agreement with the observed spectra to make definite assignments of all modes, but we have attempted a tentative explanation of the low temperature spectra.

We start with the simpler form III (Table 3, Figure 5a): comparing the positions of the three most intense calculated absorptions to the observed 7 K spectrum indicates that the harmonic frequencies are systematically overestimated. We start at the low frequency end of the spectrum, where the first sharp feature occurs at 31.2 cm^{-1}. As there should be no intramolecular vibrations in this region, we assign this to the lowest frequency calculated mode (out-of-plane dimer bending) at 37.8 cm^{-1}, whose intensity is expected to be low. The strong sharp peak at 46.1 cm^{-1} follows, which we assign to the calculated out-of-plane bending mode at 50.2 cm^{-1}. Several features are seen between 50 and 60 cm^{-1}, which most likely correspond to the weak out-of-plane twisting motion of the dimers (A_u, 51.2 cm^{-1}) and the intramolecular flexing of the 3-ring system (calculated at 55 cm^{-1} by Zeitler et al.[30]). From 68 to 90 cm^{-1}, we see four features: a strong peak at 68.4 cm^{-1}; a weaker peak at 75.5 cm^{-1}; and a strong peak at 85.9 cm^{-1} with a shoulder at 83.8 cm^{-1}. There are three calculated rigid body modes in the range, as well as the intramolecular twisting of the 3-ring system. We tentatively assign the first three observed features to the three rigid molecule modes, based on their intensities and relative frequencies, while the fourth could possibly be explained by the intramolecular vibration. (We have not calculated intensities of the phonons resulting from intramolecular modes to confirm that such an intense peak would

TABLE 3: Low Temperature ($T = 7$ K) Observed Peak Positions and Integrated Intensities of Carbamazepine Forms I and III, with Tentative Assignments Based on the Lattice Dynamics Calculations

Form III

frequency range (cm^{-1})	peak position	peak height	rel int intensity[a]	tentative assignment
29.4−33.1	31.22	0.09	0.050	out-of-plane bend (A_u, calc = 37.8 cm^{-1})
44.1−48.0	46.11	0.50	0.250	large out-of-plane bend (B_u, calc = 50.2 cm^{-1})
several features 50−60 cm^{-1}				out-of-plane twist (A_u, calc = 51.2 cm^{-1}) intramolecular: flexing of ring system (DFT on dimer: 55 cm^{-1} [30])
51.3−53.8	52.58	0.05	0.030	see above
62.6−71.7	68.40	0.86	1.000	out-of-plane twist (B_u, calc = 77.6 cm^{-1})
73.6−77.6	75.48	0.19	0.160	out-of-plane bend (A_u, calc = 78.8 cm^{-1})
79.6−83.8 (shoulder only)	83.80	0.21	0.200	out-of-plane twist (A_u, calc = 81.4 cm^{-1})
83.8−88.2 (peak without shoulder)	85.85	0.57	0.490	intramolecular: twisting of ring system (DFT on dimer: ∼90 cm^{-1} [30])
88.4−94.1 (first unresolved peak to $y = 0$)	92.94	0.38	0.440	out-of-plane twist (hidden, B_u, calc = 93.9 cm^{-1})
94.1−99.2 (second unresolved peak to $y = 0$)	96.33	0.80	0.910	2 × asymmetric stretch (B_u, calc = 104.6 cm^{-1}; A_u, calc = 118.1 cm^{-1})
99.2−105.4 (third unresolved feature)	101.46	0.50	0.520	further low-frequency intramolecular modes

Form I

frequency range (cm^{-1})	peak position	peak height	rel int intensity[a]	tentative assignment
19.9−23.0	21.46	0.20	0.003	out-of-plane twist of dimer 1; translation of dimer 2; libration of dimer 3 (A_u, calc = 24.8 cm^{-1})
23.3−27.3	25.88	0.08	0.015	mainly out-of-plane shear and twist of dimer 3 (A_u, calc = 29.0 cm^{-1})
27.6−30.5	29.06	0.04	0.005	out-of-plane twist of dimer 2; out-of-plane shear of dimer 3 (A_u, calc = 31.4 cm^{-1})
30.9−40.4 (all 3 unresolved features)	32.86	0.97	0.238	see below
30.9−34.5 (first unresolved peak)	32.86	0.97	0.139	out-of-plane twist of dimer 1; out-of-plane bend of dimer 2 (A_u, calc = 33.5 cm^{-1})
second unresolved peak	35.94	0.28		out-of-plane twist of all dimers (A_u, calc = 41.0 cm^{-1})
third unresolved peak	38.20	0.24		out-of-plane bend of dimer 1; out-of-plane twist of dimer 2 (A_u, calc = 43.4 cm^{-1})
45.0−50.1	47.34	0.37	0.070	not assigned
52.1−62.6 (both features)	55.97	0.76	0.209	not assigned
52.1−57.9 (first unresolved peak)	55.97	0.76	0.148	not assigned
57.9−62.6 (second unresolved peak)	59.56	0.33	0.061	not assigned
63.4−67.4	65.93	0.17	0.035	not assigned
69.7−78.6	72.53	0.74	0.299	not assigned
79.4−90.1 (weak shoulder included)	85.96	1.32	0.670	not assigned
91.2−108.2 (weak shoulders included)	99.10	1.54	1.000	not assigned

[a] Relative integrated intensity.

arise from such a vibration.) Between 90 and 101 cm^{-1} are three strong peaks: two of these may be due to the A_u and B_u asymmetric stretches of the dimer. The out-of-plane twisting mode calculated at 93.9 cm^{-1} is possibly too weak to be observed under these three strong peaks, in which case intramolecular vibrations are required to explain the third strong peak. If the assignments described above are correct, the rms errors in the calculated frequencies are approximately 5 cm^{-1}, in-line with typical errors for other organic molecular crystals.[22,33]

Characterization of the form I spectrum is more daunting (Table 3, Figure 5b), as there are far more visible modes, with comparable frequencies and intensities. From 21 to 33 cm^{-1}, there are three weak features followed by a strong sharp peak; the calculated spectrum has a similar pattern, so it is tempting to assign these four peaks to the first four A_u calculated modes, which predominantly involve twisting motions of the hydrogen bonding in the three dimers (Table 2). However, we must then assume that the intensity of the calculated mode at 41.0 cm^{-1} is badly overestimated to assign the two observed peaks at 35.9 and 38.3 cm^{-1} to the next two calculated frequencies. Above this, there are fewer observed features than calculated intense peaks, suggesting that many of the modes overlap in the observed spectrum. Although the individual peaks cannot be individually assigned to calculated normal modes, the calculations do provide insight into the types of vibration in the different regions of the terahertz spectrum (Figure 5b).

4. Conclusions

Harmonic lattice dynamics calculations show clear differences in the phonon spectra of the four polymorphs of carbamazepine, and analysis of the calculated eigenvectors provides an understanding of the differences in molecular motions between the forms. The variations in frequency of similar hydrogen bond

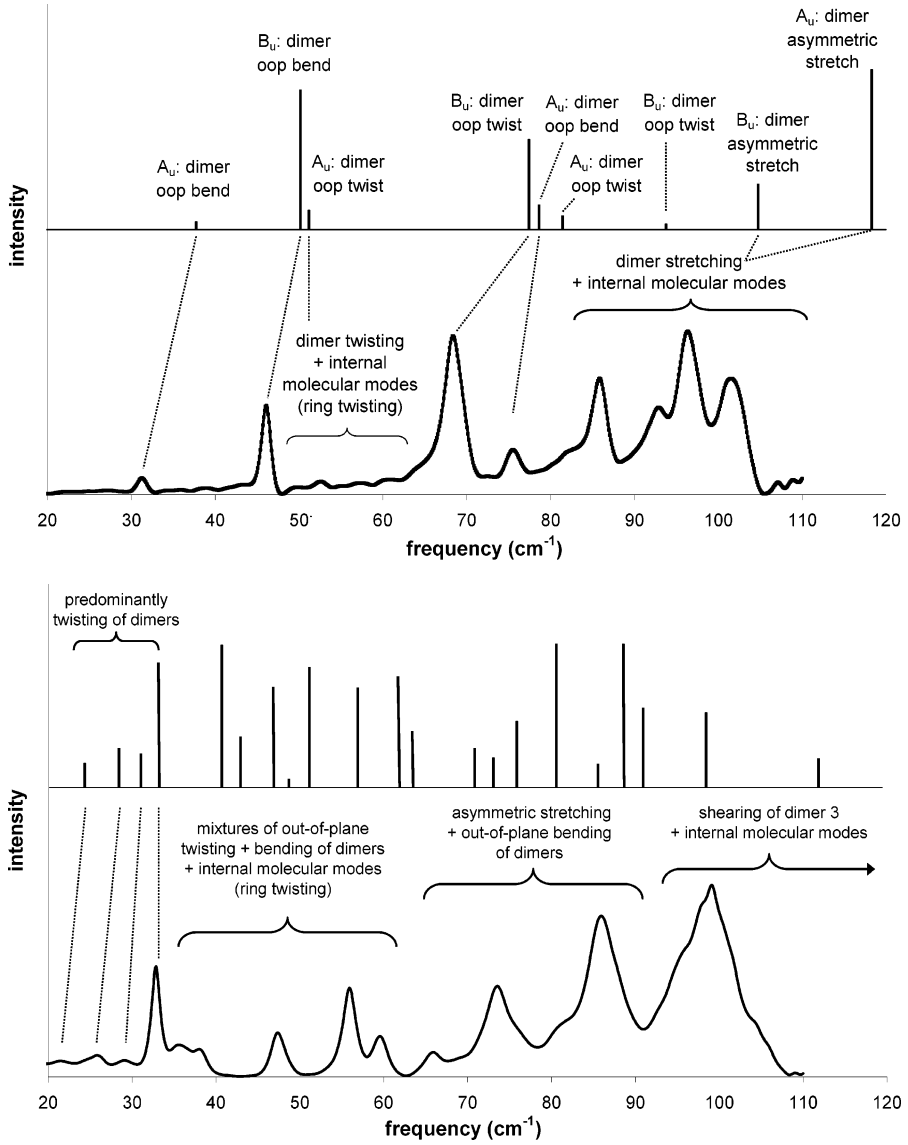

Figure 5. (a) Low temperature observed spectrum (bottom), calculated harmonic rigid molecule frequencies and intensities (top), and tentative assignments for carbamazepine form III. The observed spectrum has an empirical baseline function subtracted (oop = out-of-plane). (b) Low temperature observed spectrum (bottom), calculated harmonic rigid molecule frequencies and intensities (top), and assignment of spectral ranges for carbamazepine form I. The observed spectrum has an empirical baseline function subtracted.

vibrations between polymorphs demonstrate the influence of the crystal environment on the various types of modes, and the calculations predict similarities between the spectra of forms I and II as well as between III and IV, owing to the similar interdimer aromatic−aromatic interactions in these polymorphic pairs.

We have made tentative assignments of most features in the low temperature terahertz spectrum of carbamazepine form III and some of the lower frequency modes in the spectrum of form I. However, the agreement in both frequencies and intensities is not sufficient for these to be definitive. Several areas for improvement in calculations of phonon spectra have been highlighted. The temperature dependence of phonon modes should be developed, with the aid of variable-temperature measurements; free-energy minimization with lattice dynamics is one approach to account for the effects of thermal expansion, and anharmonic corrections can be made to the frequency calculations. Alternatively, molecular dynamics simulations offer an exact treatment of anharmonicity.[34] The explicit inclusion of temperature in simulation methods for molecular crystals will require the development of better suited model potentials, which accurately describe the temperature-free potential energy surface. Nonempirical methods for parametrizing potentials are being developed, and their use can lead to a faithful description of low temperature properties and phonon spectra.[35] Such methods should be extended to larger molecules.

The influence of molecular geometry and flexibility must be considered in the development of lattice dynamics for the interpretation of terahertz spectra. To consider the coupling of inter- and low energy intramolecular motions, potentials will need to describe molecular distortions, while not sacrificing quality in the intermolecular model. Periodic density functional theory calculations do offer one approach to treat inter- and intramolecular degrees of freedom together, though such calculations are much more costly than atomistic simulations and are subject to limitations of the chosen functional and basis set.

Despite the many necessary advances in computational methods, the present study demonstrates the usefulness of lattice dynamics calculations in explaining the terahertz spectra of molecular organic crystals and offers insight into the origin of differences between the spectra of polymorphs.

Acknowledgment. G.M.D. and W.J. thank the Pfizer Institute for Pharmaceutical Materials Science for funding. The authors thank Prof. Keith Gordon (Department of Chemistry, University of Otago) for discussions on the calculated spectra of the isolated molecule and dimer.

Supporting Information Available: Complete list of calculated frequencies for form I. This material is available free of charge via the Internet at http://pubs.acs.org.

References and Notes

(1) Strachan, C. J.; Rades, T.; Newnham, D. A.; Gordon, K. C.; Pepper, M.; Taday, P. F. *Chem. Phys. Lett.* **2004**, *390*, 20.

(2) Taday, P. F. *Philos. Trans. R. Soc. London, Ser. A* **2004**, *362*, 351.

(3) Bernstein, J. *Polymorphism in Molecular Crystals*; Clarendon Press: Oxford, 2002; Vol. 14.

(4) Fleischman, S. G.; Kuduva, S. S.; McMahon, J. A.; Moulton, B.; Bailey Walsh, R. D.; Rodriguez-Hornedo, N.; Zaworotko, M. J. *Cryst. Growth Des.* **2003**, *3*, 909.

(5) Harris, R. K.; Ghi, P. Y.; Puschmann, H.; Apperley, D. C.; Griesser, U. J.; Hammond, R. B.; Ma, C.; Roberts, K. J.; Pearce, G. J.; Yates, J. R.; Pickard, C. J. *Org. Process Res. Dev.* **2005**, *9*, 902−910.

(6) Florence, A. J.; Johnston, A.; Price, S. L.; Nowell, H.; Kennedy, A. R.; Shankland, N. *J. Pharm. Sci.*, submitted for publication, 2005.

(7) Cruz-Cabeza, A. J.; Day, G. M.; Motherwell, W. D. S.; Jones, W., in preparation, 2005.

(8) Lefebvre, C.; Guyot-Hermann, A. M.; Draguet-Brughmans, M.; Bouché, R.; Guyot, J. C. *Drug Dev. Ind. Pharm.* **1986**, *12*, 1913.

(9) McMahon, L.; Timmins, P.; Williams, A.; York, P. *J. Pharm. Sci.* **1996**, *85*, 1064.

(10) Strachan, C. J.; Taday, P. F.; Newnham, D. A.; Gordon, K. C.; Zeitler, J. A.; Pepper, M.; Rades, T. *J. Pharm. Sci.* **2005**, *94*, 837.

(11) Born, M.; Huang, K. *Dynamical Theory of Crystal Lattices*; Oxford University Press: New York, 1954.

(12) Walmsley, S. H. Basic Theory of the Lattice Dynamics of Molecular Crystals. In *Lattice Dynamics and Intermolecular Forces*; Corso, L. V., Ed.; Academic Press: New York, 1975; p 81.

(13) Califano, S.; Schettino, V.; Neto, N. *Lattice Dynamics of Molecular Crystals*; Springer-Verlag: Berlin, 1981; Vol. 26.

(14) Day, G. M. *RUDOLPh. A program for visualizing phonon modes in rigid molecular crystals*, version 1.1; Cambridge, 2005.

(15) Allen, F. H. *Acta Crystallogr.* **2002**, *B58*, 380.

(16) Grzesiak, A. L.; Lang, M.; Kim, K.; Matzger, A. J. *J. Pharm. Sci.* **2003**, *92*, 2260.

(17) Lowes, M. M. J.; Cairo, M. R.; Lotter, A. P.; van der Watt, J. G. *J. Pharm. Sci.* **1987**, *76*, 744.

(18) Reboul, J. P.; Cristau, B.; Soyfer, J. C.; Astier, J. P. *Acta Crystallogr.* **1981**, *B37*, 1844.

(19) Lang, M.; Kampf, J. W.; Matzger, A. J. *J. Pharm. Sci.* **2002**, *91*, 1186.

(20) Beyer, T.; Price, S. L. *CrystEngComm* **2000**, *2*, 183.

(21) Delley, B. *J. Chem. Phys.* **1990**, *92*, 508.

(22) Day, G. M.; Price, S. L.; Leslie, M. L. *J. Phys. Chem. B* **2003**, *107*, 10919.

(23) Williams, D. E. *J. Comput. Chem.* **2001**, *22*, 1.

(24) Williams, D. E. *J. Comput. Chem.* **2001**, *22*, 1154.

(25) Two sites were needed to describe each hydrogen atom: one for the mass and a foreshortened centre for the model potential, which is a part of the W99 parametrization.

(26) Amos, R. D.; with contributions from Alberts, I. L.; Colwell, S. M.; Andrews, J. S.; Handy, N. C.; Jayatilaka, D.; Knowles, P. J.; Kobayashi, R.; Koga, N.; Laidig, K. E.; Maslen, P. E.; Murray, C. W.; Rice, J. E.; Sanz, J.; Simandiras, E. D.; Stone, A. J.; Su, M.-D. *CADPAC*, version 6.5; Cambridge, 2001.

(27) Willock, D. J.; Price, S. L.; Leslie, M.; Catlow, C. R. A. *J. Comput. Chem.* **1995**, *16*, 628.

(28) Price, S. L.; Willock, D. J.; Leslie, M.; Day, G. M. *DMAREL*, version 3.1; 2001.

(29) Strachan, C. J.; Howell, S. L.; Rades, T.; Gordon, K. C. *J. Raman Spectrosc.* **2004**, *35*, 401.

(30) Zeitler, J. A.; Newnham, D. A.; Taday, P. F.; Strachan, C. J.; Pepper, M.; Gordon, K. C.; Rades, T. *Thermochim. Acta* **2005**, *436*, 71.

(31) Pawley, G. S.; Cyvin, S. J. *J. Chem. Phys.* **1970**, *52*, 4073.

(32) Sheka, E. F.; Bokhenkov, E. L.; Dorner, B.; Kalus, J.; Mackenzie, G. A.; Natkaniec, I.; Pawley, G. S.; Schmelzer, U. *J. Phys. C: Solid State Phys.* **1984**, *17*, 5893.

(33) Pertsin, A. J.; Kitaigorodskii, A. I. *The Atom-Atom Potential Method. Applications to Organic Molecular Solids*; Springer-Verlag: Berlin, 1987; Vol. 43.

(34) Gray, A. E.; Day, G. M.; Leslie, M.; Price, S. L. *Mol. Phys.* **2004**, *102*, 1067.

(35) Day, G. M.; Price, S. L. *J. Am. Chem. Soc.* **2003**, *125*, 16434.